

Diamond fragments as building blocks of functional nanostructures

Gregory C. McIntosh,¹ Mina Yoon,² Savas Berber,² and David Tománek²

¹Defence Technology Agency, Naval Base, Devonport, Auckland, New Zealand

²Physics and Astronomy Department, Michigan State University, East Lansing, Michigan 48824-2320, USA

(Received 12 January 2004; revised manuscript received 31 March 2004; published 2 July 2004)

Using density functional theory, we investigate the equilibrium structure, stability, and electronic properties of nanostructured, hydrogen-terminated diamond fragments. The equilibrium atomic arrangement and electronic structure of these nanostructures turn out to be very similar to bulk diamond. We find that such diamondoids may enter spontaneously into carbon nanotubes. Polymerization inside a nanotube is favored especially when boron and nitrogen are substituted for carbon atoms.

DOI: 10.1103/PhysRevB.70.045401

PACS number(s): 81.07.-b, 73.22.-f, 68.65.-k, 61.46.+w

I. INTRODUCTION

In his inspiring presentation entitled “There is Plenty of Room at the Bottom”¹ in 1959, Richard Feynman pointed out the untapped potential of functional nanostructures, assembled with atomic precision, to influence our every-day life. In the meantime, technological progress has been associated with a continuous drive towards miniaturization. Recent progress in nanoscale electromechanical systems (NEMS’s) suggests that complex functional nanostructures, invisible to the naked human eye, may soon follow suit.² Large-scale production of such complex nanostructures is likely to occur by hierarchical self-assembly from well-defined structural building blocks,^{3,4} which can be thought of as “nano-LEGO”. To fulfill their mission, such nanostructures must be strong and chemically inert in their environment.

Carbon fullerenes⁶ and nanotubes⁷ have emerged as promising candidates for such building blocks, providing a

variety of functionalities. Here, we investigate a new class of carbon nanostructures, the diamondoids.⁵ These nanoscale building blocks are very different, but compare well in stability and light weight with fullerenes and nanotubes. Being essentially hydrogen-terminated nanosized diamond fragments, they may occur in a large variety of shapes, as shown in Fig. 1. The smallest possible diamondoid is adamantane,⁸ consisting of 10 carbon atoms arranged as a single diamond cage,⁹ surrounded by 16 hydrogen atoms, as shown in Fig. 1(a). Larger diamondoids^{10–12} are created by connecting more diamond cages and are categorized according to the number of diamond cages they contain. The diamondoids shown in Fig. 1 contain up to tens of carbon atoms and are only a few nanometers in diameter.

Traditionally, diamondoids have been known in the oil industry,^{13,14} where they occur naturally dissolved in oil and its distilled by-products. At low temperatures and low pressures, diamondoids may precipitate from the solution and act as nucleation sites for the formation of sludge, which often blocks pipelines.^{15,16} Only recently, isomerically pure diamondoids with up to 11 adamantane cages have been extracted from the sludge⁵ and are now being considered for nanotechnology applications. The isolated diamondoids occur in very different shapes, and many of them form molecular crystals. These uncommon organic molecules can be chemically functionalized by substituting carbon or hydrogen atoms at the surface by other atoms or groups to promote the formation of specific polymers.

Given that diamondoids are essentially hydrogen-terminated diamond fragments, we anticipate that in the absence of significant structural changes, they share the toughness and insulating properties with their bulk diamond counterpart. Our study confirms this anticipation. In the following, we carry out a theoretical investigation of diamondoids using *ab initio* density functional calculations. We determine their equilibrium geometry, in particular the dependence of the bond lengths and bond angles on the system size, and their electronic density of states (DOS).

Beyond identifying the properties of unmodified isolated diamondoids, we also explore ways to manipulate them and to connect them together. We find that the interaction between unmodified diamondoids is too weak and does not favor polymerization to larger structures. Hence, we explore the possibility of creating specific binding sites by atomic

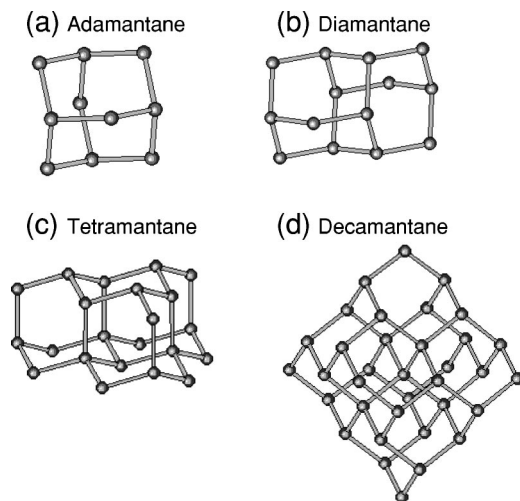


FIG. 1. Relaxed structures of lower diamondoids, identified experimentally in Ref. 5. Hydrogen atoms, terminating the carbon skeleton, are omitted from the diagrams for clarity. (a) The smallest diamondoid, adamantane, consisting of a single diamond cage. (b) Diamantane with two diamond cages. (c) Tetramantane with four diamond cages. (d) Decamantane with ten diamond cages.

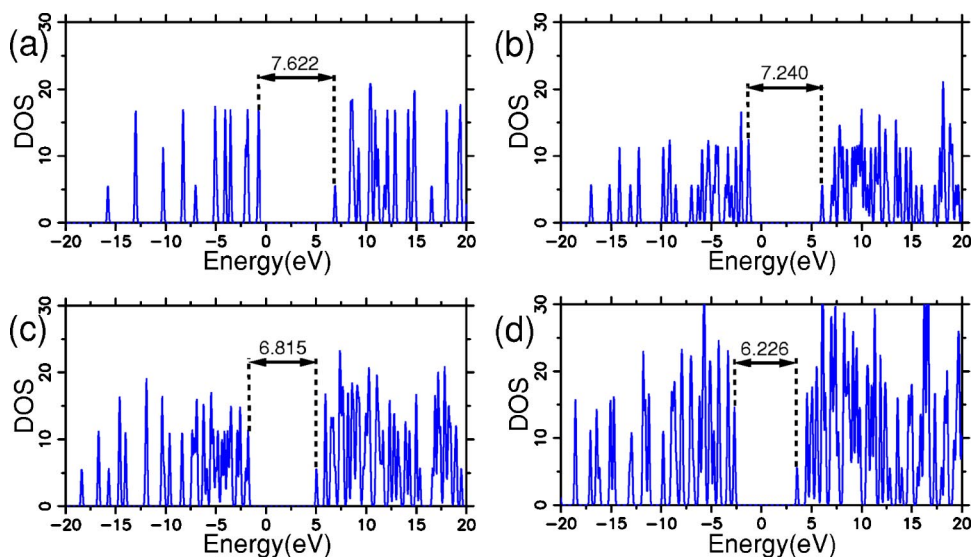


FIG. 2. (Color online) Electronic structure of an (a) adamantane, (b) diamantane, (c) tetramantane, and (d) decamantane, depicted in Fig. 1. $E=0$ corresponds to the Fermi level. The fundamental band gaps are indicated in eV.

substitution. We then explore the interaction between unmodified and functionalized diamondoids. In particular cases, we conclude that a nanotube attached to the tip of a scanning probe microscope could also be used to manipulate diamondoids into position on a substrate, similar to the way this was achieved for adsorbed rare-gas atoms.¹⁷

Even more intriguing is the possibility to use a nanotube as a container for unmodified and functionalized diamondoids, very much the same as it acts for fullerenes¹⁸ and polymers.¹⁹ The nanotube surrounding the encapsulated diamondoids may act as a template to connect these molecules in a well-defined way. In particular, we could envisage the polymerization of quasilinear polymantanes to an infinite diamondoid wire, enclosed in a nanotube.

II. METHOD OF CALCULATION

Our calculations are based on the *ab initio* density functional theory (DFT) within the local density approximation (LDA). We use Troullier-Martins pseudopotentials to describe the effect of atomic nuclei plus core electrons on the valence electrons and the Perdew-Zunger-parametrized exchange-correlation potential, as implemented in the SIESTA code.²⁰ We used a double- ζ basis²¹ and 50 Ry as the energy cutoff in plane-wave expansions of the electron density and potential, which is sufficient to achieve a total energy convergence of $\lesssim 1$ meV per atom during the self-consistency iterations.

We performed a full optimization of diamondoid structures C_nH_m containing up to ten diamond cages. Our optimized geometries, some of which are reproduced in Fig. 1, are in good agreement with those inferred experimentally^{5,22} and theoretically.^{23,24} Also, our calculated equilibrium C-C bond length of 1.540 Å in the optimized bulk diamond structure was found to agree with the experimental value.²⁵ Constrained geometries were used when determining the interaction between diamondoids.²⁶

III. PROPERTIES OF ISOLATED DIAMONDIDS

The lower diamondoids we considered here include adamantane, diamantane, triamantane, all four isomers of tetra-

mantane, all nine isomers of pentamantane with a molecular weight of 344 amu, six isomers of hexamantane, two isomers of heptamantane, and one isomer each of octamantane, nonamantane, and decamantane. With increasing polymantane size, the number of isomers increases geometrically, making an exhaustive study of all isomers impractical.⁵ In our selection of isomers, we focused on those identified experimentally in Ref. 5. For each of these diamondoids, we have de-

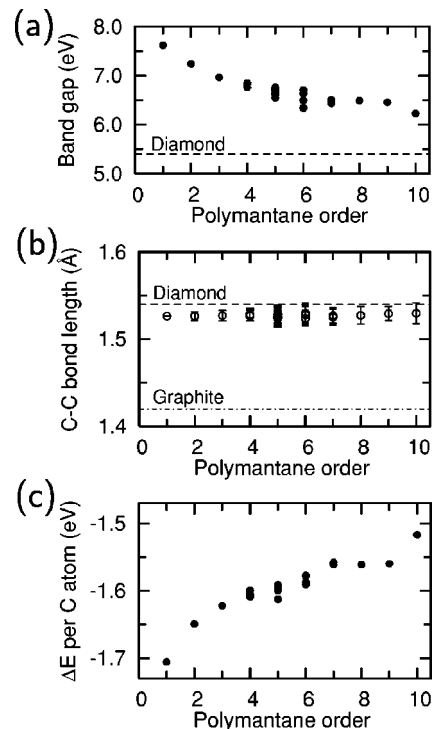


FIG. 3. Electronic, structural, and cohesive properties of diamondoid isomers considered here as a function of the polymantane order, reflecting the number of adamantane cages. (a) HOMO-LUMO gaps in the density of states (DOS). (b) C-C bond lengths, with the error bar reflecting the spread of the values within each system. (c) Formation energy per carbon atom $\Delta E/n$ of the C_nH_m diamondoids.

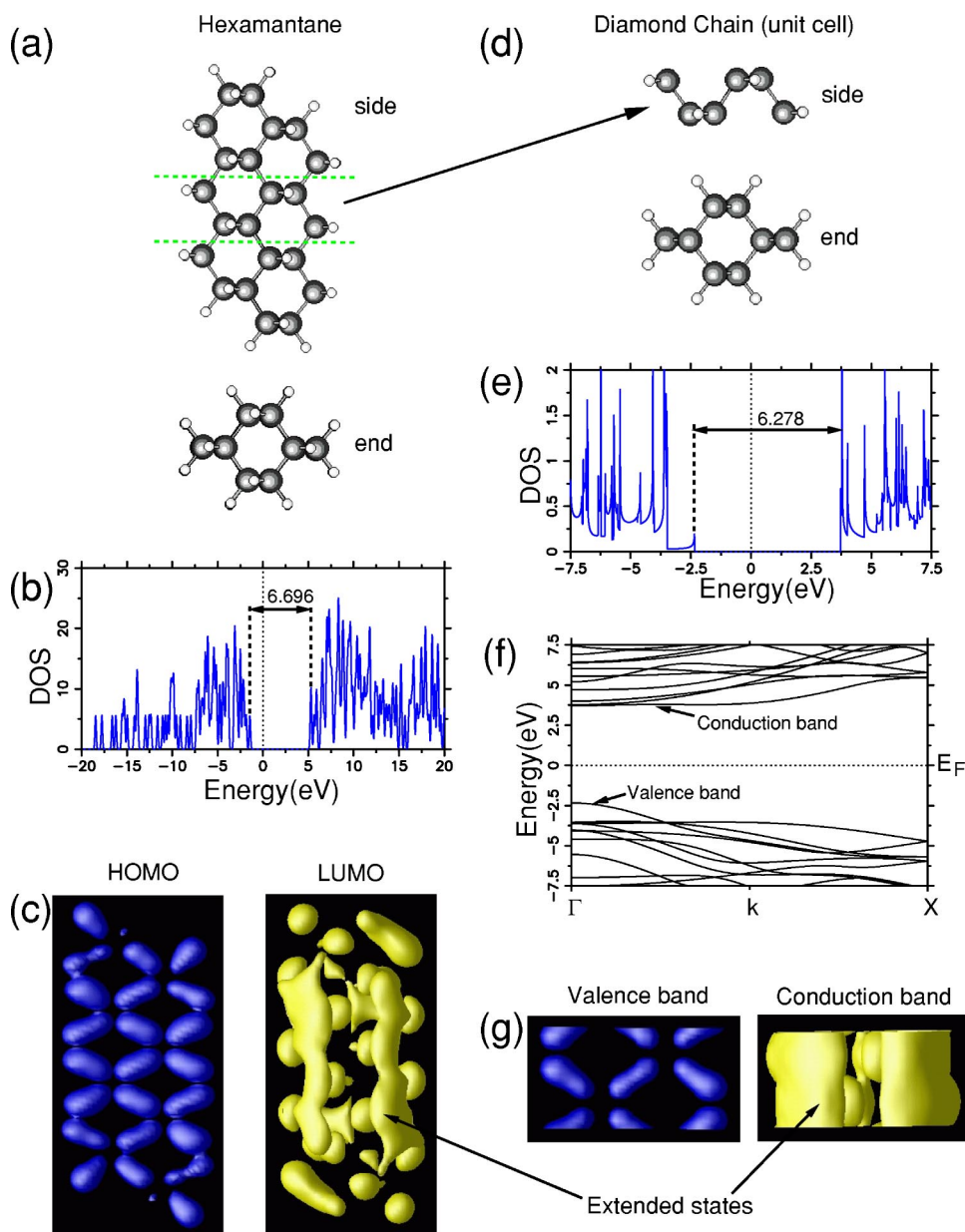


FIG. 4. (Color online) Comparison between structural and electronic properties of an elongated hexamantane isomer (left panels) and an infinite diamondoid chain (right panels). The equilibrium structure is shown in (a) and (d), with the large spheres denoting carbon and the small spheres hydrogen atoms. The electronic density of states is presented in (b) and (e), with the Fermi level at $E=0$. The one-dimensional band structure of the infinite diamondoid chain is shown in (f). The charge-distribution of electrons in the highest occupied molecular orbital (HOMO) and the lowest unoccupied molecular orbital (LUMO) of hexamantane is shown in (c). The corresponding charge distribution in the top valence and bottom conduction band of the diamondoid chain is shown in (g).

terminated the equilibrium structure, the binding energy per carbon atom, and the electronic DOS.

The electronic density of states of the diamondoids presented in Fig. 1 is shown in Fig. 2. The spectrum consists of discrete eigenvalues associated with the finite size of the molecules. With increasing size, the gap between the highest occupied molecular orbital (HOMO) and the lowest unoccupied molecular orbital (LUMO) will converge to the fundamental gap of diamond as the bulk counterpart of the finite molecules. In comparison to other atomic clusters, we find the HOMO-LUMO gap to lie very close to that of bulk diamond even for the smallest diamondoids, including adamantane, as shown in Fig. 3(a). In conjunction with the fact that the LDA usually underestimates the HOMO-LUMO gap, its large value of several electron volts suggests that diamondoids—similar to bulk diamond²⁷—should appear transparent in visible light and act as electrical insulators. This is indeed in agreement with observations in diamondoid-based molecular crystals.⁵

Figure 3 summarizes our results for the equilibrium C-C bond length, the HOMO-LUMO gap, and the formation energy per carbon atom in all the diamondoid isomers we have considered. The equilibrium C-C bond lengths in the diamondoids, depicted in Fig. 3(b), lie very close to the value found in bulk diamond. Since also the bond angles in these structures lie close to those found in diamond, we conclude that even the smallest diamondoids show sp^3 -type bonding, which is very different from graphite like sp^2 bonding found in fullerenes and nanotubes. Only in the smaller diamondoids, including adamantane, diamantane, and triamantane, is the C-C bond length somewhat smaller than in bulk diamond, reflecting the small difference between the C-H and C-C(sp^3) bonds in hydrogen-terminated carbon atoms. The error bars shown reflect mainly the differences between the inequivalent sites in the lower diamondoids and an estimated uncertainty resulting from our optimization procedure in the larger structures. In agreement with related theoretical studies,^{23,24} we find the hydrogen-terminated small diamon-

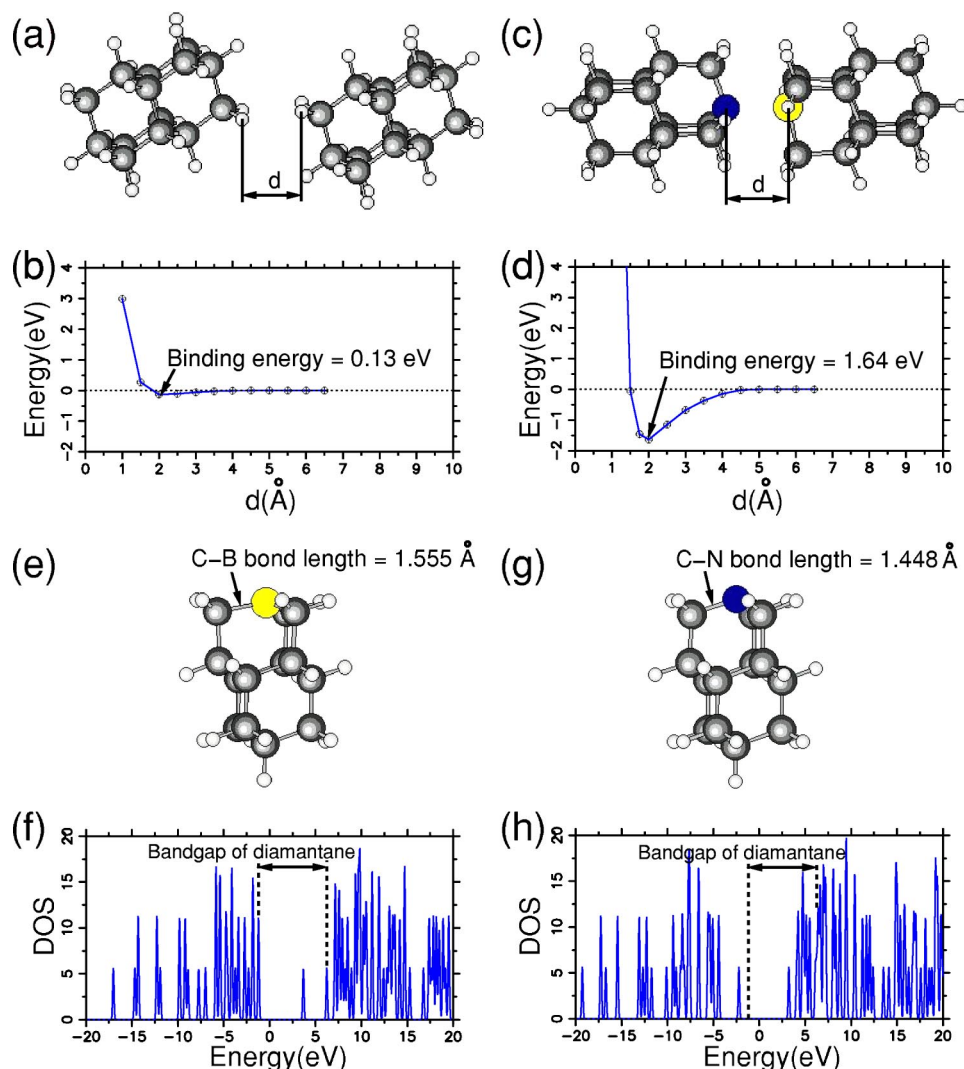


FIG. 5. (Color online) Structure, interaction energy, and electronic properties of unmodified and functionalized diamondoids. (a) Structural arrangement and (b) interaction energy of two unmodified diamondoids $C_{14}H_{20}$, separated by distance d . (c) Structural arrangement and (d) interaction energy of two chemically functionalized diamondoids $C_{13}BH_{19}$ and $C_{13}NH_{19}$, with the B and N sites in the neighboring molecules facing each other. (e) Equilibrium structure and (f) density of states of $C_{13}BH_{19}$. (g) Equilibrium structure and (h) density of states of $C_{13}NH_{19}$. The dashed lines indicate the position of the HOMO and LUMO in the unmodified diamondane, shown in Fig. 2(b). Boron (light shading) and nitrogen (dark shading) sites are emphasized in (c), (e), and (g).

doids, investigated here, stable with respect to hydrogen desorption and surface reconstruction.

The structural resemblance between even the smaller diamondoids and diamond suggests that these nanostructures will also share the desirable toughness and insulating properties with bulk diamond. The latter is indeed the case, as suggested by the large HOMO-LUMO gap we find in all the diamondoids investigated here, shown in Fig. 3(a). In agreement with former studies,^{23,24} we find the HOMO-LUMO gap to decrease monotonically with increasing diamondoid size. Among the different isomers of a particular polymantane, we can observe a subtle trend, which correlates the more elongated structures with somewhat larger HOMO-LUMO gaps than more compact structures.

Figure 3(c) shows the formation energy per carbon atom, $\Delta E/n$, of the C_nH_m diamondoids as a function of the diamondoid size. We define the formation energy by $\Delta E/n(C_nH_m) = [E_{tot}(C_nH_m) - nE_{tot}(C) - (m/2)E_{tot}(H_2)]/n$, where $E_{tot}(C)$ is the total energy of diamond per atom and $E_{tot}(H_2)$ is the total energy of a hydrogen molecule.²⁸

According to Fig. 3(c), we find all diamondoids, as well as bulk diamond, overbound due to underestimating the total energy of isolated atoms, a well-documented shortcoming of

the LDA. As suggested by the results in Fig. 3(c), the stability of the lower polymantanes is inferior to bulk diamond, since a significant fraction of carbon atoms is connected to fewer than four carbon neighbors. An intriguing observation is that the stability is nearly independent of the stacking arrangement of adamantane cages, suggesting an isomer-independent binding energy. With increasing size, we observe a monotonic increase in stability towards the bulk diamond value.

The properties of an elongated hexamantane isomer and an infinite diamondoid chain as its quasi-one-dimensional (quasi-1D) crystalline counterpart are discussed in Fig. 4. Such structural elements could find use in NEMS devices and, as we discuss in the following sections, could be self-assembled inside carbon nanotubes. Figures 4(a) and 4(d) show the close structural relationship between the finite molecule and the infinite chain, obtained by periodically repeating the unit cell shown in Fig. 4(d). The average C-C bond length in the infinite diamondoid chain is 1.530 ± 0.008 Å, close to the values found for the other diamondoids, given in Fig. 3(b).

The electronic density of states of hexamantane is shown in Fig. 4(b). In all respects, including its large HOMO-LUMO gap, this DOS lies close to the results found in the

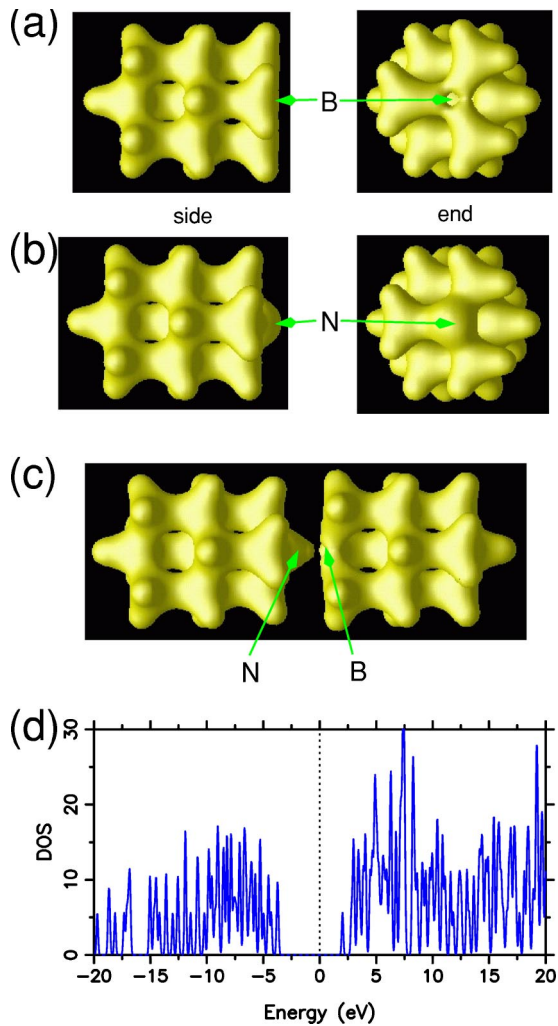


FIG. 6. (Color online) Total charge distribution in (a) $C_{13}BH_{19}$ and (b) $C_{13}NH_{19}$ in their equilibrium structure, shown in Figs. 5(e) and 5(g). (c) Total charge distribution and (d) electronic density of states of $C_{13}BH_{19}$ interacting with $C_{13}NH_{19}$ in the structural arrangement depicted in Fig. 5(c).

other diamondoids, depicted in Fig. 2. The electronic spectrum of the infinite quasi-1D counterpart of hexamantane, shown in Fig. 4(e), is similar to that of hexamantane and dominated by a series of van Hove singularities in the valence and conduction regions. The dense sequence of these singularities reflects the dense spectrum of relatively flat bands, depicted in Fig. 4(f), which makes this system a wide-gap insulator with an indirect gap. In view of the negative electron affinity of diamond,²⁹ combined with a large length-to-diameter aspect ratio, diamondoid chains may even surpass carbon nanotubes in applications such as cold cathodes or low-voltage electron emitters in flat panel displays.

In spite of its wide fundamental gap, the infinite diamondoid chain could possibly acquire conductivity by electron or hole doping. Close inspection of the electronic dispersion relations in Fig. 4(f) reveals that the bands close to the Fermi level show an energy dispersion of below 2 eV. To investigate the charge delocalization as a prerequisite for conduction, we display the charge distribution of the topmost valence and bottom conduction bands in Fig. 4(g) and compare

it to that of the HOMO and LUMO of hexamantane in Fig. 4(c).

Results for the infinite chain suggest that the charge associated with the valence band is localized in pockets near interatomic bonds, thus hindering hole transport. This charge distribution is very similar to that of the HOMO of hexamantane. The conduction band, on the other hand, consists of four strongly delocalized states located on the outer perimeter of the structure, which could be used to conduct electrons. These extended conduction states find their counterpart in the LUMO of hexamantane, which is similarly delocalized across the middle section of this molecule. The bottom of the conduction band is very flat, suggesting that electrons in a lightly electron-doped system should have a low mobility.

Due to the wide fundamental gap, chemical doping is unlikely to provide free carriers, since it would require the introduction of impurities with a very low ionization potential, likely to introduce trap sites. One possibility of electron doping would involve gating a supported diamondoid chain. A more likely scenario of n doping would involve enclosing the diamondoid chain inside a carbon nanotube, as discussed below, and n doping the surrounding nanotube.

IV. FUNCTIONALIZED DIAMONDOIDS

Construction of functional elements of diamondoid-based NEMS devices precludes a controllable method to connect diamondoids with strong bonds. Chemically unmodified diamondoids interact only weakly, leading to the formation of molecular crystals.⁵ This is illustrated in Figs. 5(a) and 5(b), showing the arrangement and binding of two interacting diamondoid cages.³⁰ The binding energy of two diamondoids, only 0.13 eV in our calculation, is to be considered only a rough estimate and lower limit on the real value, mainly due to the structural constraints imposed in our calculation.²⁶ Still, identifying ways to stabilize the bond is desirable.

One way to enhance bonding involves chemical functionalization of diamondoids in order to create more reactive sites. Obvious choices for substitution are elements close to carbon in the periodic table, such as boron and nitrogen, which have a similar atomic size as carbon. We also note that carbon has been successfully replaced by boron and nitrogen in fullerenes and carbon nanotubes.³¹ A similar substitution of terminal carbon atoms by boron and nitrogen in adjacent diamondoids, shown in Fig. 5(c), should result in a much stronger polar bond between the modified molecules. This is indeed confirmed by our results shown in Fig. 5(d). Even though significantly smaller than the typical bond energy in diamond, the binding energy²⁶ of 1.64 eV between the functionalized diamondoids should prevent spontaneous dissociation at room temperature.

Our results for functionalized diamondoids are summarized in Figs. 5(e)–5(h). We find that substituting a CH group in $C_{14}H_{20}$ by either a boron or a nitrogen atom leads to stable structures, with a geometry closely related to that of unmodified diamondoid. In $C_{13}BH_{19}$, depicted in Fig. 5(e), the C-B bond length is somewhat larger than the C-C bond length, suggesting a weaker bond. In $C_{13}NH_{19}$ on the other hand, shown in Fig. 5(g), the C-N bond is shorter than the C-C

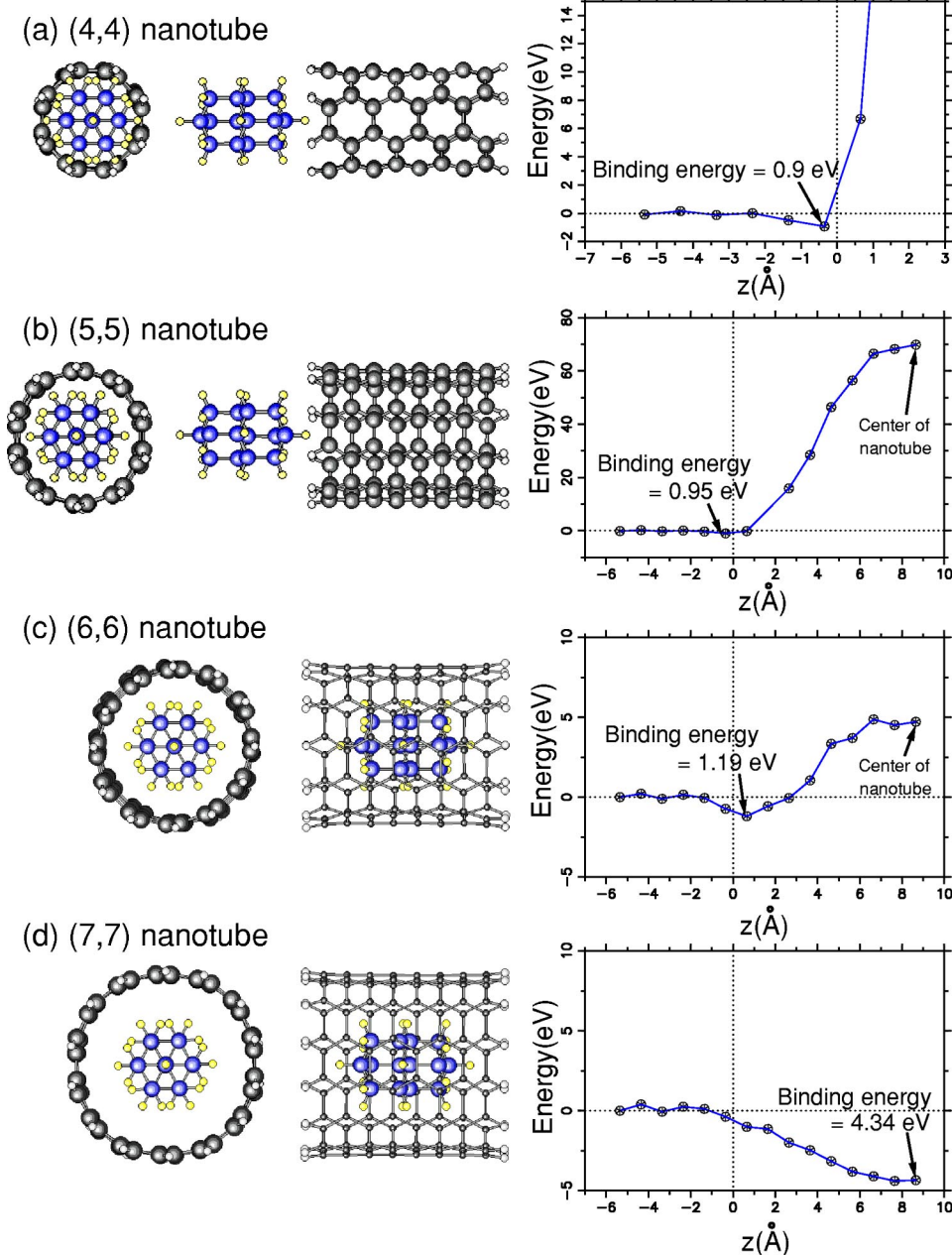


FIG. 7. (Color online.) Energetics of a diamantane molecule entering (n,n) carbon nanotubes with various diameters. The end-on and side views of the insertion geometry are depicted in the left panels. The axial separation between the closest end of the diamantane and the nanotube is denoted by z , with $z < 0$ corresponding to the diamantane outside and $z > 0$ to the diamantane inside the carbon nanotube.

bond, suggesting a stronger bond. Substitution of a carbon atom by either boron or nitrogen leads in both cases to impurity states within the HOMO-LUMO gap of their density of states, shown in Figs. 5(f) and 5(h).

The effect of atomic substitution on the overall charge distribution within the functionalized diamondoids is shown in Fig. 6. The Periodic Table would suggest a charge depletion at the boron site and a charge accumulation at the nitrogen site. This is indeed confirmed in Fig. 6(a) for $C_{13}BH_{19}$ and in Fig. 6(b) for $C_{13}NH_{19}$.

Combining the excess charge at the nitrogen site in $C_{13}NH_{19}$, clearly visible by a charge density protrusion in Fig. 6(b), with a charge deficit at the boron site in $C_{13}BH_{19}$, visible in Fig. 6(a), leads to the formation of a polar bond, once the two sites face each other. As seen in Fig. 6(c), we find the charge cloud at the nitrogen site further extended towards the positively charged boron site in the stable com-

plex consisting of the two functionalized diamondoids. Close inspection of the charge density distribution in the bond region also illustrates the fundamental difference between the weaker, predominantly polar B-N bond, with very little charge in the bond region, and covalent C-C bonds with a strong charge accumulation in the bond region.

Similar to the individual functionalized diamondoids, also the bonded complex shows a large HOMO-LUMO gap of few eV in the density of states, as seen in Fig. 6(d). Due to the polar nature of the bond, the total density of states of the complex is closely related to that of its components, shown in Figs. 5(f) and 5(h).

V. INTERACTION OF DIAMANTOIDS WITH CARBON NANOTUBES

Since the cross section of carbon nanotubes is compatible with the size of diamondoids, nanotubes could be used to

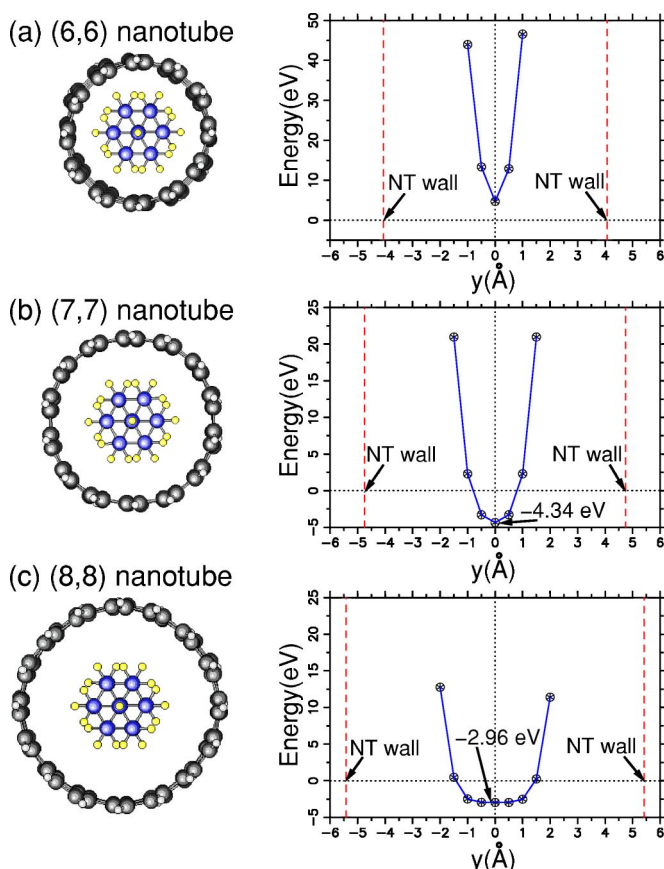


FIG. 8. (Color online) Energetics of diamantane, enclosed inside a (6,6), (7,7), and (8,8) carbon nanotube, as a function of an off-axis displacement y . The geometry in end-on view is shown in the left panels.

manipulate and assemble these molecules to larger structures. Precise deposition and positioning of diamondoids could be achieved with the help of a carbon nanotube attached to the tip of a scanning probe microscope,^{17,32} which may combine its functionality as a storage, deposition, and manipulation device. Combination of diamondoids with nanotubes may, moreover, lead to functional nanostructures for particular applications. Key to all these applications is to understand the interaction of diamondoids with carbon nanotubes.

In the following, we describe the interaction of diamantane as a prototype diamondoid with (n,n) armchair carbon nanotubes of different diameter. Aspects of particular interest to us are the energy change associated with the entry of a diamondoid inside a nanotube and the optimum nanotube diameter to maximize the encapsulation energy.

Our results for the entry of diamantane into armchair carbon nanotubes ranging from (4,4) to (7,7) are presented in Fig. 7. Due to computer limitations, we considered finite-length nanotube segments, which have been hydrogen terminated at both ends. The encapsulation geometry is depicted in end-on and side views in the left panels of Fig. 7. The dependence of the diamantane-nanotube interaction energy on the diamantane position z along the tube axis is presented in the right panels of Fig. 7.

These energy results suggest that entry of diamantane into a (4,4), (5,5), and (6,6) nanotube is energetically unfavorable. Nevertheless, the dip in the total energy at $z \approx 0$ suggests the possibility of attaching this molecule to the hydrogen-terminated nanotube end and thus a possibility of manipulating diamondoids with a nanotube attached to an SPM tip. In all cases, the diamantane-nanotube binding energy is lower than the bond strength between $C_{13}BH_{19}$ and $C_{13}NH_{19}$, shown in Fig. 5(d), suggesting the possibility to manipulate and position assemblies of connected, functionalized diamondoids without disrupting them.

As seen in Fig. 7, only (n,n) nanotubes with $n \geq 7$ are wide enough to accommodate diamantane endohedrally without energy investment. The energy of diamantane encapsulated inside wider (n,n) nanotubes is shown in Fig. 8 as a function of its off-axis displacement y . We find that the (7,7) nanotube has an ideal diameter to contain a single diamantane with optimal encapsulation energy. Containment in the (6,6) nanotube is moderately endothermic. Containment in the (8,8) nanotube is exothermic, but the minimum in the energy curve is rather flat, suggesting that the diamondoid would have some degree of lateral freedom and that the (8,8) nanotube is too wide. Nevertheless, the enclosing nanotube should suppress free rotation of the diamondoid, thus facilitating specific reactions, including polymerization addressed in Fig. 5. Results very similar to those for diamantane are also expected for all higher, linear diamondoids, as well as the diamond chain, addressed in Fig. 4. The encapsulation of the smaller adamantane should proceed very similar to that of diamantane, with the exception that orientational alignment of adamantane with no obvious “long” axis cannot be achieved.

VI. SUMMARY AND CONCLUSIONS

In summary, we performed *ab initio* density functional calculations to study the structural and electronic properties of unmodified and chemically functionalized polymantanes, as well as their reactivity and interaction with carbon nanotubes. Our results support the conjecture that the lower polymantanes are essentially hydrogen-terminated diamond fragments with diamondlike properties. Hence, these systems may be used as molecular building blocks of complex functional nanostructures, to be found in future NEMS devices. Within computational uncertainty, we find the bond lengths and angles in the carbon skeletal structure of the diamondoids to be essentially the same as in bulk diamond. The similarity in bonding between diamondoids and diamond extends also to the bond strength and resistance to deformations. The large HOMO-LUMO gaps in diamondoids are the molecular counterparts of a large fundamental gap in diamond, which is responsible for its optical transparency in the visible range and its insulating properties. We also find the properties of hydrogen-terminated diamondoids to approach those of bulk diamond, as their size increases.

Unmodified diamondoids are nonreactive and interact only weakly with each other. We found, however, that substituting carbon by boron and nitrogen atoms may create localized binding sites in these modified diamondoids and

provide the possibility of connecting diamondoids by much stronger, directional bonds. Selective substitution at more than one carbon site per diamondoid may provide the possibility to connect even larger diamondoids into well-defined nanostructures for particular applications.

We have found that diamondoids should enter spontaneously into carbon nanotubes with a wide enough diameter, similar to the spontaneous encapsulation of fullerenes, leading to peapods.¹⁸ Being orientationally constrained in these nanosized containers, they may fuse into long structures, including a “diamond wire.” Carbon nanotubes can be used not only to store diamondoids, but also to manipulate them sterically, preferably in conjunction with a scanning probe micro-

scope. Even nanotubes that are too narrow to contain a diamondoid may be used for such a purpose, since diamondoids preferentially bind to the reactive open end of a nanotube, which may be attached to the tip of a scanning probe microscope.

ACKNOWLEDGMENTS

We thank W. Qureshi, J. E. Dahl, S. G. Liu, and R. M. Carlson for drawing our attention to their results prior to publication. We also thank Noejung Park and Eiji Osawa for useful discussions. This work has been partly supported by NSF-NIRT Grant No. DMR-0103587.

-
- ¹Presentation of Richard P. Feynman at the annual meeting of the American Physical Society at the California Institute of Technology on December 29, 1959. Reprinted in *The Pleasure of Finding Things Out*, edited by J. Robbins (Perseus Books, New York, 1999).
- ²K. E. Drexler, *Sci. Am. (Int. Ed.)* **285**, 74 (2001).
- ³G. I. Leach and R. C. Merkle, *Nanotechnology* **5**, 168 (1994).
- ⁴G. Leach, *Nanotechnology* **7**, 197 (1996).
- ⁵J. E. Dahl, S. G. Liu, and R. M. K. Carlson, *Science* **299**, 96 (2003).
- ⁶H. W. Kroto, J. R. Heath, S. C. O'Brien, R. F. Curl, and R. E. Smalley, *Nature (London)* **318**, 162 (1985).
- ⁷S. Iijima, *Nature (London)* **354**, 56 (1991).
- ⁸P. R. von Schleyer, *J. Am. Chem. Soc.* **79**, 3292 (1957).
- ⁹W. H. Bragg and W. L. Bragg, *Nature (London)* **91**, 554 (1913).
- ¹⁰C. Cupas, P. R. von Schleyer, and D. J. Trecker, *J. Am. Chem. Soc.* **87**, 917 (1965).
- ¹¹V. Z. Williams, Jr., P. R. von Schleyer, G. J. Gleicher, and L. B. Rodewald, *J. Am. Chem. Soc.* **88**, 3362 (1966).
- ¹²D. Farcasiu, H. Bohm, and P. R. von Schleyer, *J. Org. Chem.* **42**, 96 (1977).
- ¹³G. A. Mansoori, *J. Pet. Sci. Eng.* **17**, 101 (1997).
- ¹⁴D. Vazquez Gurrola, J. Escobedo, and G. A. Mansoori, “*Characterization of Crude Oils from Southern Mexican Oil Fields*,” in EXITEP 1998 Proceedings, Mexico City, Mexico.
- ¹⁵J. Reiser, E. McGregor, J. Jones, R. Enick, and G. Holder, *Fluid Phase Equilib.* **117**, 160 (1996).
- ¹⁶J. E. Dahl, J. M. Moldowan, K. E. Peters, G. E. Claypool, M. A. Rooney, G. E. Michael, M. R. Mello, and M. L. Kohnen, *Nature (London)* **399**, 54 (1999).
- ¹⁷D. M. Eigler and E. K. Schweizer, *Nature (London)* **344**, 524 (1990); J. A. Stroschio and D. M. Eigler, *Science* **254**, 1319 (1991).
- ¹⁸B. W. Smith, M. Monthieux, and D. E. Luzzi, *Nature (London)* **396**, 323 (1998).
- ¹⁹G. C. McIntosh, D. Tománek, and Y. W. Park, *Phys. Rev. B* **67**, 125419 (2003).
- ²⁰P. Ordejón, E. Artacho, and J. M. Soler, *Phys. Rev. B* **53**, R10441 (2000); D. Sánchez-Portal, P. Ordejón, E. Artacho, and J. M. Soler, *Int. J. Quantum Chem.* **65**, 453 (1997).
- ²¹We found a significant energy difference between the presently used double- ζ and the minimum basis set. Based on calculations for the related ethylene molecule, using a triple- ζ basis would change the binding energy per atom by $\lesssim 3$ meV.
- ²²R. H. Boyd, S. N. Sanwal, S. Shary-Tehrany, and D. McNally, *J. Phys. Chem.* **75**, 1264 (1971).
- ²³J. Y. Raty, G. Galli, C. Bostedt, T. W. van Buuren, and L. J. Terminello, *Phys. Rev. Lett.* **90**, 037401 (2003).
- ²⁴J. Y. Raty and G. Galli, *Nat. Mater.* **2**, 792 (2003).
- ²⁵C. Kittel, *Introduction to Solid State Physics* (Wiley, New York, 1996).
- ²⁶To limit the computational effort associated with a large number of degrees of freedom, we kept the atomic arrangement within interacting diamondoids frozen in the optimum geometry when determining the total energy of the interacting system. Due to the suppression of relaxations, our estimates provide only a lower limit on the binding energy.
- ²⁷C. E. Nebel, *Semicond. Sci. Technol.* **18**, S1 (2003).
- ²⁸We use the values $E_{\text{tot}}(\text{C}) = -154.35$ eV for the total energy of diamond per atom and $E_{\text{tot}}(\text{H}_2) = -30.54$ eV for the total energy of a hydrogen molecule, based on the same computational approach and basis as applied to the diamondoids.
- ²⁹Johan F. Prins, *Semicond. Sci. Technol.* **18**, S125 (2003).
- ³⁰To limit the computational effort, we chose diamantane as a representative of elongated building blocks.
- ³¹D. Golberg, Y. Bando, W. Han, K. Kurashima, and T. Sato, *Chem. Phys. Lett.* **308**, 337 (1999).
- ³²Y. Nakayama, H. Nishijima, S. Akita, K. I. Hohmura, S. H. Yoshimura, and K. Takeyasu, *J. Vac. Sci. Technol. B* **18**, 661 (2000).